ARMY RESEARCH LABORATORY

Carbon Nanotube/Graphene Supercapacitors Containing Manganese Oxide Nanoparticles

by Matthew Ervin, Vinay Raju, Mary Hendrickson, and Thomas Podlesak

ARL-TR-6289 **December 2012**

NOTICES

Disclaimers

The findings in this report are not to be construed as an official Department of the Army position unless so designated by other authorized documents.

Citation of manufacturer's or trade names does not constitute an official endorsement or approval of the use thereof.

Destroy this report when it is no longer needed. Do not return it to the originator.

Army Research Laboratory
Adelphi, MD 20783-1197

ARL-TR-6289 **December 2012**

Carbon Nanotube/Graphene Supercapacitors Containing Manganese Oxide Nanoparticles

Matthew Ervin and Vinay Raju
Sensors and Electronic Devices Directorate, ARL

Mary Hendrickson and Thomas Podlesak
Command, Power, and Integration Directorate, CERDEC

REPORT DOCUMENTATION PAGE	Form Approved OMB No. 0704-0188

1. REPORT DATE *(DD-MM-YYYY)*	2. REPORT TYPE	3. DATES COVERED (From - To)
December 2012	Final	October 2011 to September 2012

4. TITLE AND SUBTITLE
Carbon Nanotube/Graphene Supercapacitors Containing Manganese Oxide Nanoparticles

5a. CONTRACT NUMBER

5b. GRANT NUMBER

5c. PROGRAM ELEMENT NUMBER

6. AUTHOR(S)
Matthew Ervin, Vinay Raju, Mary Hendrickson, and Thomas Podlesak

5d. PROJECT NUMBER

5e. TASK NUMBER

5f. WORK UNIT NUMBER

7. PERFORMING ORGANIZATION NAME(S) AND ADDRESS(ES)
U.S. Army Research Laboratory
ATTN: RDRL-SER-L
2800 Powder Mill Road
Adelphi, MD 20783-1197

8. PERFORMING ORGANIZATION REPORT NUMBER
ARL-TR-6289

9. SPONSORING/MONITORING AGENCY NAME(S) AND ADDRESS(ES)

10. SPONSOR/MONITOR'S ACRONYM(S)

11. SPONSOR/MONITOR'S REPORT NUMBER(S)

12. DISTRIBUTION/AVAILABILITY STATEMENT
Approved for public release; distribution unlimited.

13. SUPPLEMENTARY NOTES

14. ABSTRACT
Supercapacitors are of interest because they are energy storage devices with greater power density than batteries. Unfortunately, supercapacitors have significantly lower energy densities than batteries, which limit the applications for supercapacitors. The addition of pseudocapacitance, that is, chemical reactions similar to those in batteries but which behave electrically like a capacitance, can be used to increase the energy density of supercapacitors. This work focuses on increasing the capacitance of carbon nanotube (CNT)- or graphene-based supercapacitors by adding pseudocapacitive manganese oxide nanoparticles. A number of methods have been investigated for fabrication of CNT/graphene/manganese oxide composites. Manganese oxide nanoparticle pseudocapacitance has been successfully incorporated into CNT/graphene-based supercapacitors. Further optimization of the composite compositions and electrode fabrication methods is still required to optimize the energy densities of these devices.

15. SUBJECT TERMS
Supercapacitor, CNT, graphene, manganese oxide, pseudocapacitance

16. SECURITY CLASSIFICATION OF:			17. LIMITATION OF ABSTRACT	18. NUMBER OF PAGES	19a. NAME OF RESPONSIBLE PERSON
a. REPORT	b. ABSTRACT	c. THIS PAGE			Matthew Ervin
Unclassified	Unclassified	Unclassified	UU	22	19b. TELEPHONE NUMBER (*Include area code*) (301) 394-0017

Standard Form 298 (Rev. 8/98)
Prescribed by ANSI Std. Z39.18

Contents

List of Figures iv

1. Introduction 1

2. Results 2

2.1 GO/Manganese Acetate Solution Preparation....2

2.2 G/MnOx NP Synthesis Method Investigation....3

2.2.1 Dry Mixing/Grinding....3

2.2.2 Solution Mixing Synthesis....3

2.2.3 Freeze-dry Synthesis....4

2.2.4 Hydrothermal Processing....5

2.2.5 Spray Dry Processing....6

2.3 Capacitor Performance....7

2.3.1 Capacitor Evaluation....7

2.3.2 Capacitance Increasing with Cycling....8

2.3.3 Morphology Change with Cycling....9

2.3.4 Mechanically Unstable Electrodes....9

2.3.5 Greater Capacitance at Slower Scan Rate....10

2.3.6 Electrolyte Effects....11

2.3.7 Pseudocapacitance Results....12

3. Conclusions 12

4. References 14

List of Symbols, Abbreviations, and Acronyms 15

Distribution List 16

List of Figures

Figure 1. TGA at 1 °C/min of MnAc demonstrating that it decomposes below 300 °C. The mass lost indicates that Mn_3O_4 may be the resulting species. 2

Figure 2. SEM image of ball milled MnAc (3 mole %) with multi-wall carbon nanotubes (MWCNTs) annealed at 370 °C. The resulting material is rather inhomogeneous and the MnOx NPs do not appear to be well associated with the MWCNTs (Mn370C303).....3

Figure 3. SEM image of ball milled MnAc (3 mole %) with MWCNTs annealed at 370 °C. The resulting material is rather inhomogeneous and the MnOx NP do not appear to be well associated with the MWCNTs (Mnsoln370107). 4

Figure 4. SEM of rGO coated with MnOx nanoparticles fabricated through freeze-dry method (VNRA1).....5

Figure 5. Hydrothermally produced MnOx NPs on CNTs (left) and rGO (right) (MnHTCNT204, MnHTG205). 5

Figure 6. SEM images of reduced, drop-cast GO solution (left) and reduced, spray-dried GO solution (right) (MHE23502 and MHE23802). 6

Figure 7. SEM of MnOx NPs formed on rGO using spray dry process (SDGO14, SDGO09).....7

Figure 8. Representative CV scan of a rGO/MnOx NP electrode in 0.5 M K_2SO_4.....7

Figure 9. Depiction of 1200 CV cycles of a spray-dried MWCNT/MnOx NP electrode made with Kynar 761 binder. The red trace is the first cycle (MHE23403). 8

Figure 10. SEM image of MWCNT/MnOx NP electrode after 9000 CV cycles showing MnOx NP platelet formation. (MHE20001). 9

Figure 11. SEM of spray-dried rGO nanosphere electrode with 20% SWCNT as binder (MHE24303). 10

Figure 12. Plot of capacitance observed as a function of scan rate (MHE25406). 11

Figure 13. CV curves of a rGO/MnOx NP electrode in K_2SO_4 (left), NaCl (middle), and $CaCl_2$ (right) (MHE25402, 04, 05). 11

1. Introduction

Supercapacitors have several advantages over conventional batteries, including higher specific power (~2 orders of magnitude higher), higher cycle life (millions of charge/discharge cycles), rapid charge/discharge times (seconds to minutes), high efficiencies (up to 98%), and good performance in extreme heat and cold (*1*). Increasing supercapacitor energy and power densities will make them more useful for portable power applications. Two materials being studied for supercapacitor electrodes are single-wall carbon nanotubes (SWCNTs) and graphene (G). Extremely large double-layer capacitances may be obtainable if these materials can be assembled in a manner that optimizes the electrode surface area that is accessible to the electrolyte.

Solution-based processing was chosen for this work as it is manufacturable and it does not impose significant thermal and chemical constraints on the underlying current collector as direct growth on the current collector would. When carbon nanotubes (CNTs) or G are deposited from solution, they typically do so in bundles or as stacked sheets. Our previous work (*2*) indicates that this bundling or restacking is detrimental to the resulting accessible surface area and therefore reduces the double-layer capacitance.

In this work, the addition of manganese oxide nanoparticles (NPs) to the CNTs or G surfaces has been investigated to see if it increases the capacitances of these materials. Approaches to deposit the NPs onto the CNTs/G before electrode fabrication, as opposed to electrochemically depositing the NPs onto an existing CNT/G electrode, were investigated as there was a possibility that deposition onto existing CNT/G electrodes would prevent the incorporation of NPs within the CNT bundles or between stacked G sheets. This is important since the inclusion of NPs is, in part, desirable as it may prevent the tight bundling/restacking of the CNTs/G, thus increasing the accessible surface area, which would increase the specific double-layer capacitance of these materials. In addition, manganese oxide is known to have pseudocapacitive properties (*3*). That is, it supports fast redox reactions that behave like a capacitance. Such redox-based capacitance would impart an additional pseudocapacitance contribution to the specific capacitances of the CNT/G electrodes. The CNT/G material, in turn, increases the electrical conductivity of the manganese oxide (MnOx), which increases the electrochemical utility of this material.

A number of fabrication methods for combining CNT or G with MnOx NPs are investigated here. While incorporation of MnOx NPs may increase energy density through increased accessible surface area and pseudocapacitive contributions, the NPs may also reduce the power density by reducing the electrode electronic conductivity, and it may reduce the cycle life

through the incorporation of redox reactions. Characterization of these materials has uncovered a number of issues that will need to be addressed in a practical device.

2. Results

2.1 GO/Manganese Acetate Solution Preparation

Numerous electrodes were made using CNTs in powder form and graphene oxide (GO) solution obtained from commercial sources (Helix Material Solutions and Cheaptubes.com, respectively). The benefit of working with GO is that it is water soluble and once the electrode has been fabricated, the GO can be thermally reduced to graphene (G, or rGO). Typically, 225 °C overnight (in air) has been used to thermally reduce the GO used here. The thermal conversion of manganese acetate (MnAc) (obtained from Sigma Aldrich) has been used to produce the MnOx NPs used here (*3*). Higher temperatures (300 °C/1 h/in air) have typically been used to convert the MnAc to MnOx. Thermal gravimetric analysis (TGA) was used to determine that the MnAc decomposes below 300 °C, as shown in figure 1. The amount of mass lost indicates that Mn_3O_4 may be the resulting species. The electrode materials produced were examined with scanning electron microscopy (SEM).

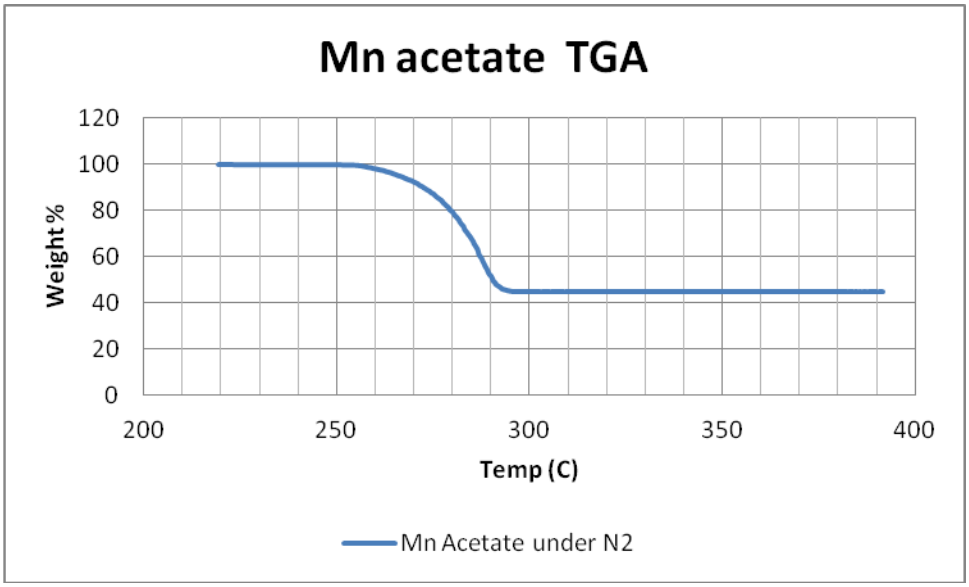

Figure 1. TGA at 1 °C/min of MnAc demonstrating that it decomposes below 300 °C. The mass lost indicates that Mn_3O_4 may be the resulting species.

2.2 G/MnOx NP Synthesis Method Investigation

2.2.1 Dry Mixing/Grinding

Dry mixing and grinding of CNTs with MnAc was attempted as described by Yi Lin (*4*). After baking the dry mixture, SEM imaging indicated there was insufficient mixing of the materials and that using more than 5 mole % of MnAc may be useful, as can be seen in figure 2.

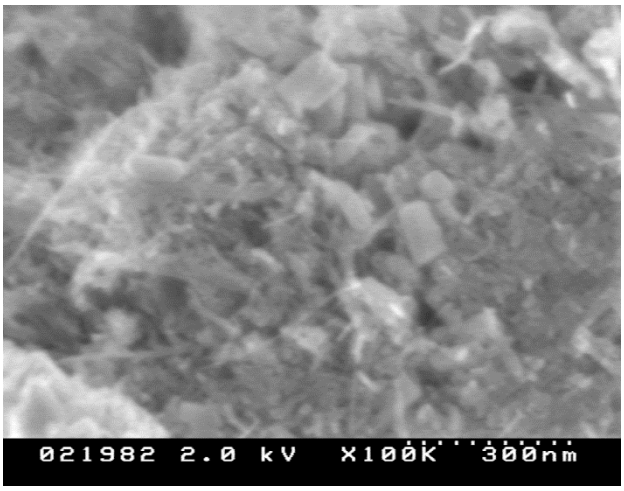

Figure 2. SEM image of ball milled MnAc (3 mole %) with multi-wall carbon nanotubes (MWCNTs) annealed at 370 °C. The resulting material is rather inhomogeneous and the MnOx NPs do not appear to be well associated with the MWCNTs (Mn370C303).

2.2.2 Solution Mixing Synthesis

In order to obtain a more thorough mixing of the CNTs and MnAc, a mixing of these materials in solution was attempted. A mass ratio of 18:82 MnAc:MWCNT was suspended in ethanol (the MnAc dissolves, but the MWCNTs are merely suspended). The resulting suspension was immediately drop cast after ultrasonication and the resulting deposit was baked at 370 °C. As can be seen in figure 3, 10-nm NPs are associated with the MWCNTs, but there are also agglomerated MnOx NPs. The lack of complete mixing of the materials is likely due to separation during the dropcasting.

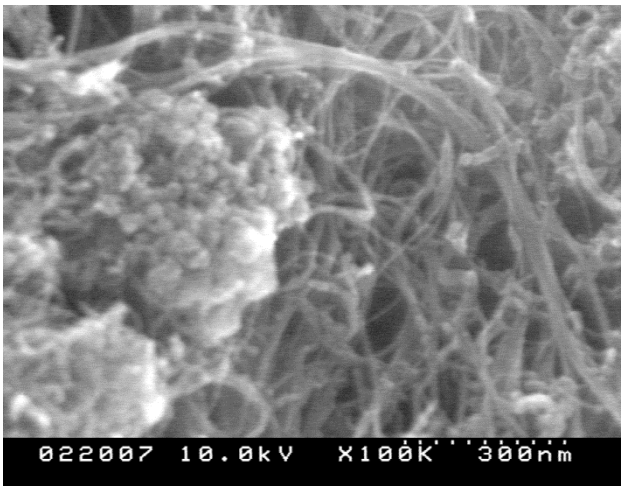

Figure 3. SEM image of ball milled MnAc (3 mole %) with MWCNTs annealed at 370 °C. The resulting material is rather inhomogeneous and the MnOx NP do not appear to be well associated with the MWCNTs (Mnsoln370107).

2.2.3 Freeze-dry Synthesis

In an effort to prevent the segregation of the MnAc from the carbon during evaporation of the solution, a freeze dry method was used. In addition, a water solution of GO was used for the carbon source since the GO is actually in solution and not merely suspended as the MWCNTs above were. Next, 2 mg of GO and 3.3 mg of MnAc were dissolved in 3 ml of water. This solution was flash frozen by depositing it drop wise into liquid nitrogen. The resulting ice crystals were freeze dried at 10^{-3} torr. After baking to reduce the GO to rGO and convert the MnAc to MnOx, the resulting powder was imaged with the SEM. Figure 4 shows there are small MnOx NPs coating the rGO. While successful in producing NP-coated graphene, it was difficult to collect sufficient material for further electrode processing, so additional synthesis methods were attempted.

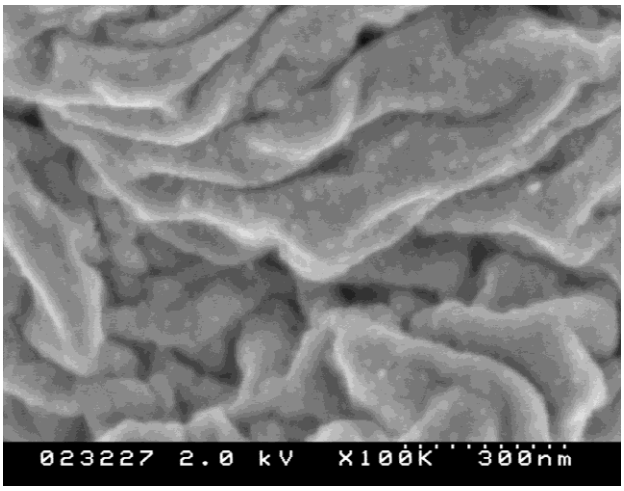

Figure 4. SEM of rGO coated with MnOx nanoparticles fabricated through freeze-dry method (VNRA1).

2.2.4 Hydrothermal Processing

Next, 2 to 1 solutions (by mass) of MnAc and CNTs or GO were hydrothermally treated at 200 °C for 14 h and the resulting MnOx NP decorated materials are seen in figure 5.

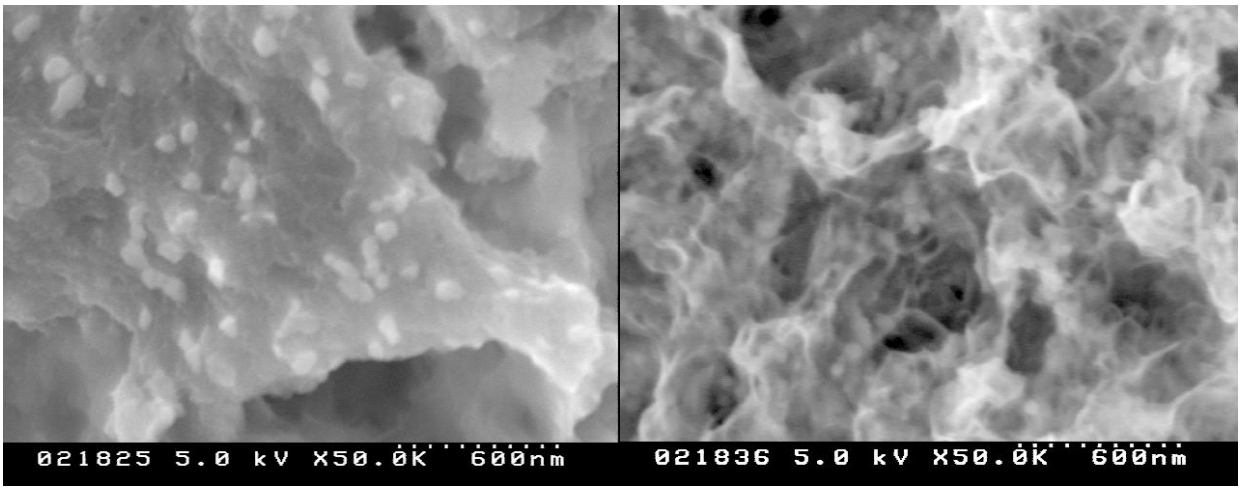

Figure 5. Hydrothermally produced MnOx NPs on CNTs (left) and rGO (right) (MnHTCNT204, MnHTG205).

For subsequent hydrothermal syntheses, a MnAc and GO solution was mixed with trace amounts of potassium hydroxide (KOH) using a procedure described by Wang (*5*). The fabrication process involved stirring 0.4 mmol MnAc solution, 0.9 mmol KOH solution, and GO solution (1 mg/mL) and heating at 180 °C for 14 h in a Teflon-coated autoclave. The solution was then deposited onto current collectors by dropcasting. These electrodes were then baked at 300 °C for 1 h to ensure that the MnAc was converted to MnOx NPs.

2.2.5 Spray Dry Processing

The final synthesis method investigated was spray drying, which was done with the assistance of Prof. Hongwei Qiu of Stevens Institute of Technology. As it turns out, spray drying has some interesting effects on the GO all by itself even before MnAc is incorporated. In spray drying, the GO solution is aerosolized and the droplets are dried with a hot carrier gas. The surface tension of the drying droplets, crumples the GO sheets up into nanospheres. Figure 6 shows the flat uncrumpled appearance of drop cast GO solution and the crumpled morphology of the spray dried GO solution. The crumpled morphology is of interest for further investigation since it may result in more surface area and greater ionic conductivity (porosity) in the electrodes produced this method. On the other hand, the crumpled morphology will increase the electrical resistivity due to reduced contact between adjacent rGO sheets in the final electrode.

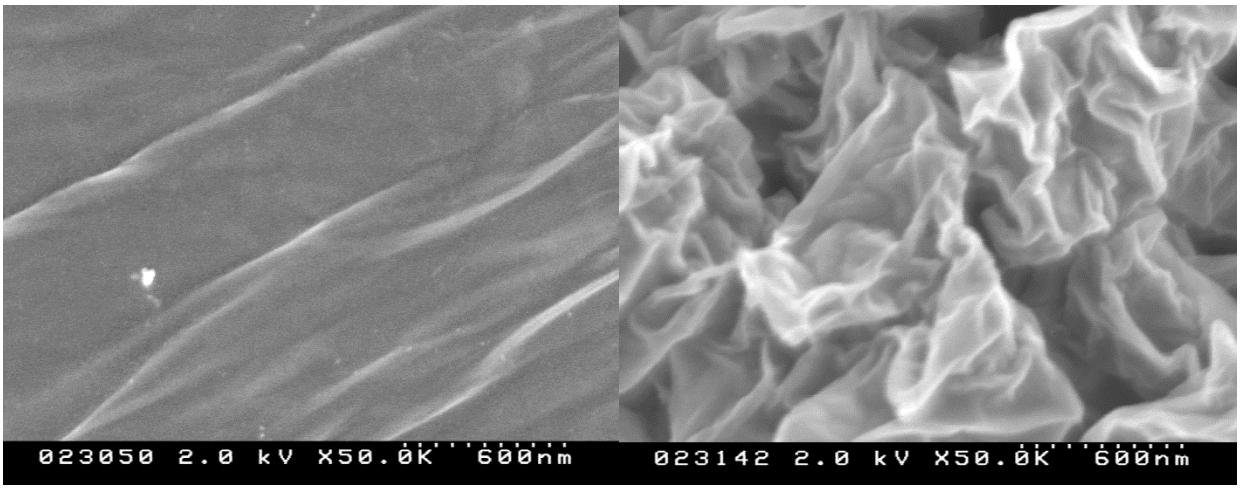

Figure 6. SEM images of reduced, drop-cast GO solution (left) and reduced, spray-dried GO solution (right) (MHE23502 and MHE23802).

When MnAc is included with GO in the spray-dried solution, a good mixture of the MnOx NP and rGO sheets results, as can be seen in figure 7. The figure shows 5- to 10-nm NPs on the rGO.

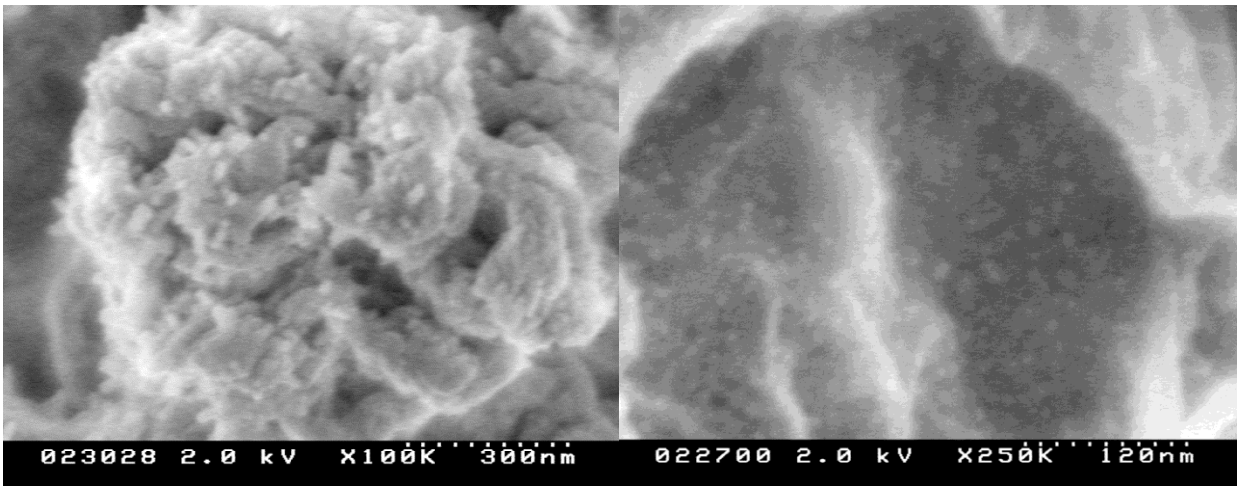

Figure 7. SEM of MnOx NPs formed on rGO using spray dry process (SDGO14, SDGO09).

2.3 Capacitor Performance

2.3.1 Capacitor Evaluation

Electrodes were fabricated by drop casting solutions containing the GO/CNT/MnAc materials onto titanium (Ti) or stainless steel current collectors and then annealing them to reduce the GO or convert the MnAc to MnOx as needed. Testing was performed using cyclic voltammetry (CV) and electrochemical impedance spectroscopy (EIS) on a potentiostat typically using a three-electrode setup with a large excess of electrolyte. In a later experiment, a two electrode setup was used with fabricated button cells. The CV scan rate for the majority of the testing was 20 mV/s, except where noted. The voltage range of scan was 0 to 0.7 V (versus the silver/silver chloride electrode when using the three electrode mode). The electrolyte typically used in this study was 0.5 M potassium sulfate (K_2SO_4). A typical CV obtained is seen in figure 8.

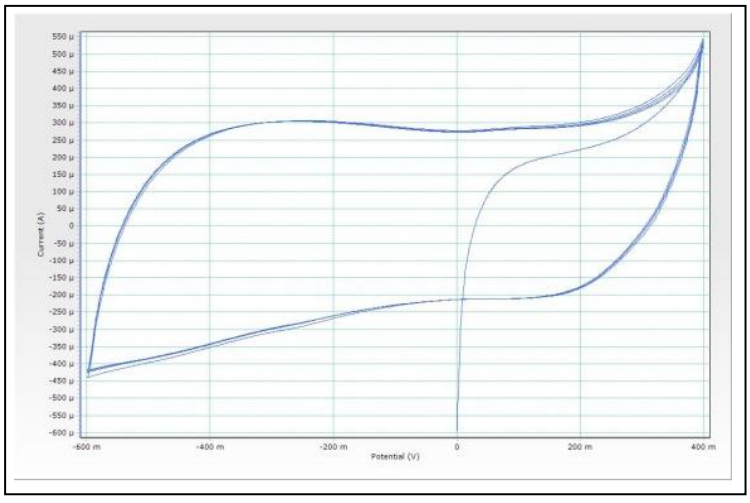

Figure 8. Representative CV scan of a rGO/MnOx NP electrode in 0.5 M K_2SO_4.

The specific capacitance is calculated from a three electrode measurement using

$$CV\ Current/(Scan\ Rate*Mass\ of\ Sample) = Capacitance\ (F/g) \quad (1)$$

where the current is measured as half the difference between the oxidation and reduction currents near the center of the CV curve near where this value is a minimum to avoid overstating the capacitance. In a two electrode (button cell) measurement, the specific capacitance is calculated in the same manner, but the mass of both electrodes is included and the result is multiplied by four to report it in the three electrode standard as is observed in the literature.

2.3.2 Capacitance Increasing with Cycling

A MnOx NP decorated MWCNT material was made using a spray-dry process. This electrode material was deposited onto a current collector from an n-methylpyrrolidone (NMP) suspension that also contained polyvinylidene fluoride (PVDF) binder. When this electrode was cycled for 1200 cycles, the capacitance was observed to increase from 29.2 to 42.8 mF, as shown in figure 9. After subtracting out the capacitance expected from the MWCNTs alone, the specific capacitance of the MnOx NPs was calculated to increase from 8.3 to 31.8 F/g. It is believed that this increase is due to the conversion of the MnOx from its initially synthesized phase believed to be Mn_3O_4 to the more electrochemically active birnessite phase (*6*).

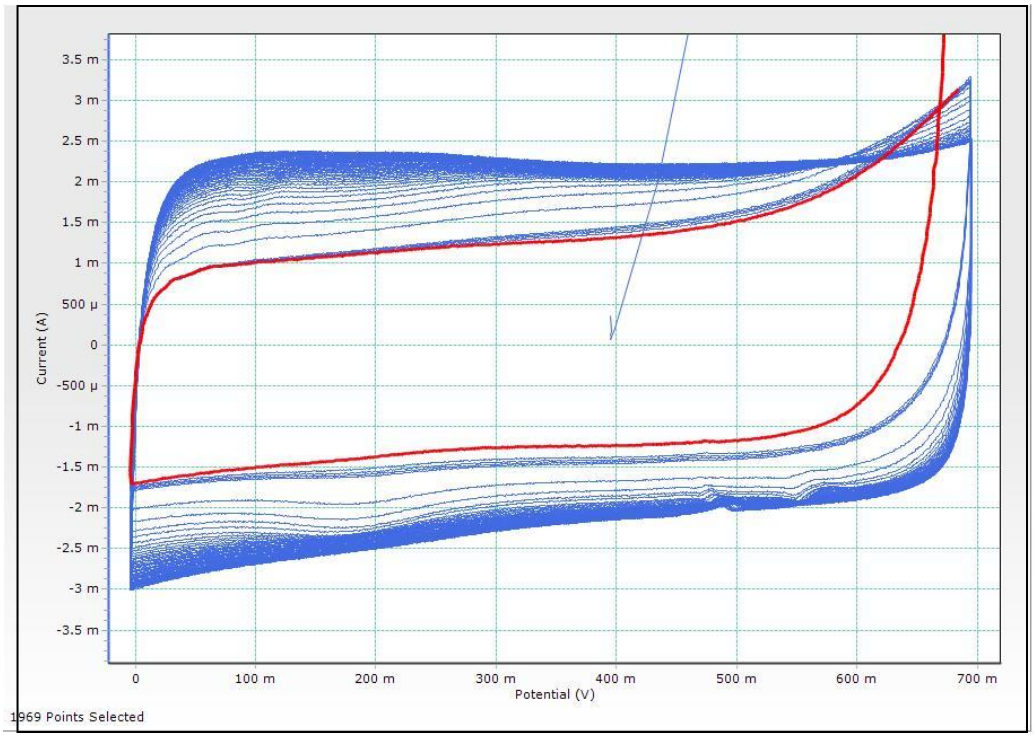

Figure 9. Depiction of 1200 CV cycles of a spray-dried MWCNT/MnOx NP electrode made with Kynar 761 binder. The red trace is the first cycle (MHE23403).

2.3.3 Morphology Change with Cycling

Unfortunately, the capacitance does not always increase with cycling. Often, it decreases for various reasons. There may be a potential issue with the MnOx dissolving during part of the CV cycle and then redepositing later in the cycle. Figure 10 shows the morphology of the MnOx NP after 9000 cycles. In this case, the capacitance was still increasing, but the significant changes in morphology could be an issue in a practical device. Since the MnOx dissolves during part of the CV cycle, it is possible that the electrodes tested in a three electrode mode using a large excess of electrolyte could lose a significant amount of Mn to the electrolyte. However, making a button cell with a limited amount of electrolyte was not successful in increasing the measured capacitance, so this may not be a serious issue with the measurements made here.

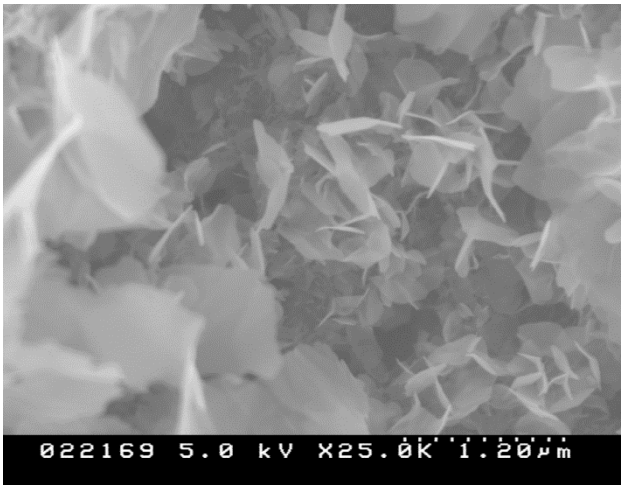

Figure 10. SEM image of MWCNT/MnOx NP electrode after 9000 CV cycles showing MnOx NP platelet formation. (MHE20001).

2.3.4 Mechanically Unstable Electrodes

The hydrothermal method used mixed KOH with MnAc and GO. The KOH seemed to have formed crystals on some of the dropcast electrodes. Here, KOH crystals were formed in the electrode and created an unstable electrode mass by absorbing moisture from the air. Dissolution of the KOH crystals also resulted in the electrode deteriorating in the electrolyte, producing falling capacitance readings.

Another potential reason for an electrode material losing electrical contact with the current collector is due to insufficient binder. In much of this work, a binder material was not used to avoid any complications that would result if it coated the surface of the electrode materials. However, electrochemical deterioration was observed when testing many electrodes, sometimes due to a detachment of the electrode material from the current collector. When necessary electrodes were made using a PVDF binder, but the formulation has not been optimized. The

CNT and G materials have such large surface areas that more binder than is typically used to make electrodes is likely required to obtain adequate mechanical robustness.

2.3.5 Greater Capacitance at Slower Scan Rate

Since redox reaction based pseudocapacitance is slower than the double-layer capacitance contribution, it is worthwhile to measure how the capacitance changes with the scan rate. The electrode used was made from spray-dried powder from a solution that had 100 mg of GO and 145 mg of MnAc in 50 ml of water, which should yield >10 mole % Mn:C. This spray-dried GO/Mn Ac powder was baked at 275 °C for 4 h. Then, 1.06 mg of the reduced/converted powder was mixed with 0.37 mg of SWCNTs in NMP. The SWCNTs were added to improve the electrical conductivity between the MnOx NP covered G nanospheres and bind the electrode materials together. Figure 11 shows a similar electrode made without the MnOx NPs.

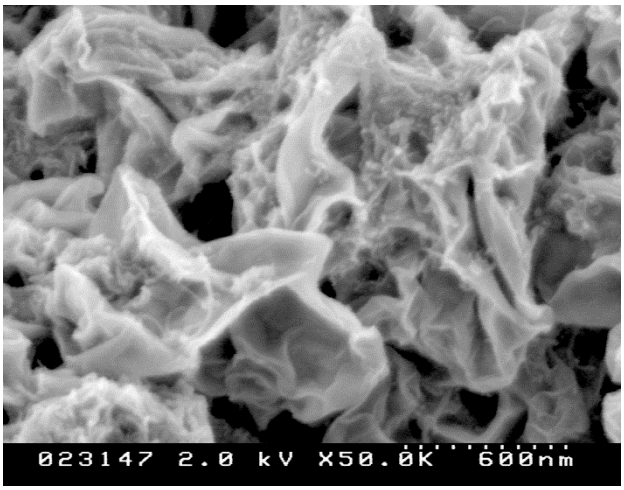

Figure 11. SEM of spray-dried rGO nanosphere electrode with 20% SWCNT as binder (MHE24303).

The resulting suspension was dropcast onto a Ti current collector. The capacitance as a function of scan rate is plotted in figure 12. At the slowest scan rate measured, 2 mV/s, the capacitance was measured to be 135 F/g.

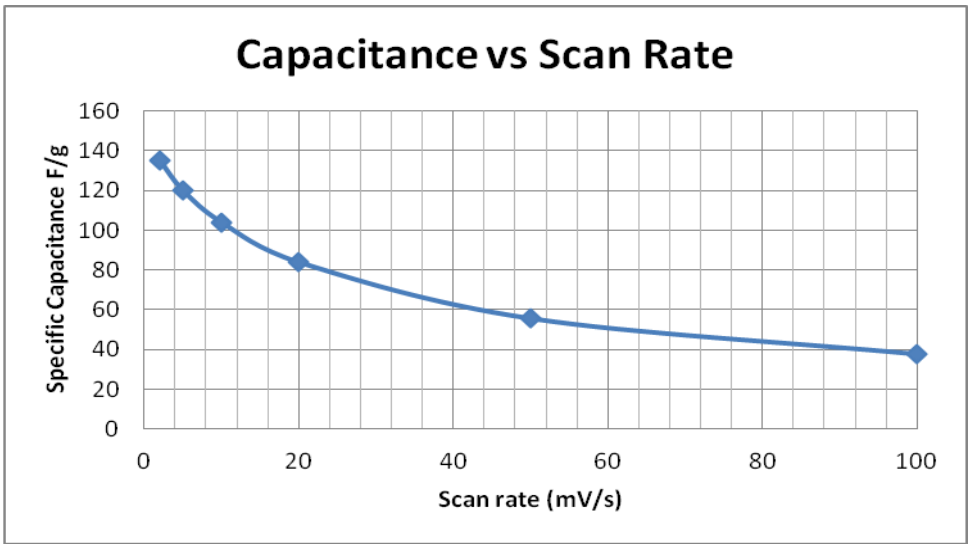

Figure 12. Plot of capacitance observed as a function of scan rate (MHE25406).

2.3.6 Electrolyte Effects

MnOx containing electrodes are typically used with neutral (pH) electrolytes. In order to investigate the effect of the electrolyte on the capacitance observed, the same spray-dried rGO/MnOx NP with SWCNT electrode as above was tested at a 2 mV/s scan rate in three different electrolytes: 0.5 M K_2SO_4, 1 M sodium chloride (NaCl), and 1 M calcium chloride ($CaCl_2$). The qualitative CV behavior of the three electrolytes can be seen in figure 13. Before taking these CVs, the electrode was cycled in 0.5 M K_2SO_4 for 200 cycles until its capacitance stabilized. Then it was tested in the three electrolytes in succession. The observed capacitances were 85.7 F/g in K_2SO_4, 97.8 F/g in NaCl, and 153 F/g in $CaCl_2$ electrolyte. These results are considered reliable, and not inflated by a leakage current, because the phase angle as measured using electrochemical impedance spectroscopy is –80° at the lowest frequency (10 mHz) measured, and so there is not a significant leakage current contributing to the measured capacitance.

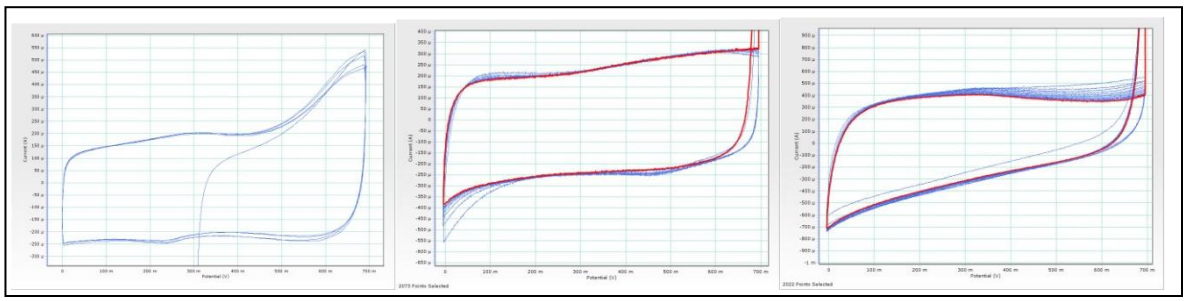

Figure 13. CV curves of a rGO/MnOx NP electrode in K_2SO_4 (left), NaCl (middle), and $CaCl_2$ (right) (MHE25402, 04, 05).

2.3.7 Pseudocapacitance Results

In the above electrolyte study, a specific capacitance of 84 F/g was obtained at 20 mV/s in $CaCl_2$ electrolyte. This is the combination of the double-layer capacitance of the SWCNTs and rGO combined with the pseudocapacitance of the MnOx NPs. Extracting the pseudocapacitance of the MnOx NPs is somewhat difficult and requires some approximations. If I assume that the GO has a C_7O_3 stoichiometry and the MnAc converts to MnO_2 and that the rGO contributes 50 F/g (based on a similar electrode with no MnOx) and the SWCNTs contribute 35 F/g (based on previous work), I then calculate the MnOx NPs are contributing 108 F/g of pseudocapacitance. This is a reasonable result when compared to the literature for MnOx electrodes (*3*), but is it lower than some reports in the literature for MnOx/G or CNT electrodes. The measured pseudocapacitance is presumably higher at the slower scan rate of 2 mV/s, but I do not have sufficient data to calculate that value at this time.

Capacitors made using the hydrothermal method from the literature did not yield specific capacitances higher than what could be achieved with rGO alone. It is possible that the 180 F/g for MnOx reported when using the hydrothermal method is in error as they used a very low MnOx loading on their G and their observed capacitance could be entirely due to the G (*5*).

3. Conclusions

In this work, a number of synthesis methods have been investigated for making MnOx NPs on CNT/G electrodes for achieving increased double-layer capacitance as well as adding pseudocapacitance to CNT/G electrodes. Some methods (dry/solution mixing) were abandoned as they did not result in sufficient mixing of the MnOx and G/CNTs. Another (freeze drying) was abandoned due to the difficulty in making sufficient material on a laboratory scale. Both hydrothermal processing and spray drying appear to be promising methods for coating G/CNTs with NPs.

In all of the methods, the decomposition of MnAc to MnOx was used to produce the MnOx NPs. Electrodes made with these composite materials were found to increase in capacitance with electrochemical cycling, which is believed to convert the initial MnOx phase to a more active phase, and it is also observed to change the morphology of the MnOx deposits. As is typical with supercapacitors, the capacitance was observed to increase as the CV scan rate was decreased. The electrolyte used was also found to significantly affect the observed capacitance with $CaCl_2$, yielding almost twice the capacitance as K_2SO_4. A specific capacitance of 108 F/g was calculated for the pseudocapacitance of the MnOx phase at 20 mV/s with more expected at slower scan rates. This is comparable to what has been reported in the literature for MnOx;

however, there have been reports of significantly higher specific capacitances for MnOx/G or CNT composite electrodes in the literature.

In future work, the best ratio of MnOx:G/CNT should be determined. In much of the reported MnOx:G/CNT composite electrode work, the G/CNT is merely an additive that increases the electrical conductivity of the MnOx. The energy and power requirements of the ultimate application are liable to determine the optimum ratio of materials. In addition, additional synthesis routes for producing the most electrochemically active MnOx phase should be investigated. Finally, more electrode fabrication process optimization is required to prevent electrode deterioration that is sometimes seen.

4. References

1. Pandolfo, G.; Hollenkamp, A. F. *J. Power Sources* **157**, 11–27 (2006).
2. Ervin, M. H.; Mailly, B.; Palacios, T. Electrochemical Double Layer Capacitance of Metallic and Semiconducting SWCNTs and Single-Layer Graphene. *ECS Transactions* **2012**, *41* (22), 153–160.
3. Xu, F.; Kang, B.; Li, B.; Du, H. Recent Progress on Manganese Dioxide Based Supercapacitors. *Journal Material Research* **2010**, *25* (8) 1421–1432.
4. Lin, Yi; Watson, K. A.; Fallbach, M. J.; Ghose, S.; Smith, J. G. Jr; Delozier, D. M.; Cao, W.; Crooks, R. E.; Connell, J. W. Rapid, Solventless, Bulk Preparation of Metal Nanoparticle-decorated Carbon Nanotubes. *ACS Nano* **2009**, *3*, 871–884.
5. Wang, D.; Li, Y.; Wang, Q.; Wang, T. Facile Synthesis of Porous Mn_3O_4 Nanocrystal-Graphene Nanocomposites for Electrochemical Supercapacitors. *Journal Inorganic Chemistry* **2012**, 628–635.
6. Inoue, R.; Nakashima, Y.; Tomono, K.; Nakayama, M. Electrically Rearranged Birnessite-Type MnO2 by Repetitive Potential Steps and Its Pseudocapacitive Properties. *Journal of the Electrochemical Society* **2012**, *159* (4), A445–A451.

List of Symbols, Abbreviations, and Acronyms

$CaCl_2$	calcium chloride
CNTs	carbon nanotubes
CV	cyclic voltammetry
EIS	electrochemical impedance spectroscopy
G or rGO	graphene
GO	graphene oxide
K_2SO_4	potassium sulfate
KOH	potassium hydroxide
MnAc	manganese acetate
MnOx	manganese oxide
MWCNTs	multi-wall carbon nanotubes
NaCl	sodium chloride
NMP	n-methylpyrrolidone
NPs	nanoparticles
PVDF	polyvinylidene fluoride
SEM	scanning electron microscopy
SWCNTs	single-wall carbon nanotubes
TGA	thermal gravimetric analysis
Ti	titanium

NO. OF COPIES	ORGANIZATION
1 ELEC	ADMNSTR DEFNS TECHL INFO CTR ATTN DTIC OCP 8725 JOHN J KINGMAN RD STE 0944 FT BELVOIR VA 22060-6218
1	US ARMY RSRCH DEV AND ENGRG CMND ARMAMENT RSRCH DEV & ENGRG CTR ARMAMENT ENGRG & TECHNLGY CTR ATTN AMSRD AAR AEF T J MATTS BLDG 305 ABERDEEN PROVING GROUND MD 21005-5001
1	US ARMY INFO SYS ENGRG CMND ATTN AMSEL IE TD A RIVERA FT HUACHUCA AZ 85613-5300
1	US GOVERNMENT PRINT OFF DEPOSITORY RECEIVING SECTION ATTN MAIL STOP IDAD J TATE 732 NORTH CAPITOL ST NW WASHINGTON DC 20402

NO. OF COPIES	ORGANIZATION
2 HCS 2 PDFS	CERDEC ATTN THOMAS PODLESAK (1 PDF 1 HCS) ATTN MARY HENDRICKSON (1 PDF 1 HCS) RDEC-CPP-PG 5100 MAGAZINE ROAD ABERDEEN PROVING GROUND MD 21005
15 HCS 1 PDF	US ARMY RSRCH LAB ATTN IMAL HRA MAIL & RECORDS MGMT ATTN RDRL CIO LL TECHL LIB ATTN RDRL SER L B PIEKARSKI ATTN RDRL SER L M DUBEY ATTN RDRL SER L M ERVIN (1 PDF 10 HCS) ATTN RDRL SER P AMIRTHARAJ ADELPHI MD 20783-1197